

RSC Advances



This is an *Accepted Manuscript*, which has been through the Royal Society of Chemistry peer review process and has been accepted for publication.

Accepted Manuscripts are published online shortly after acceptance, before technical editing, formatting and proof reading. Using this free service, authors can make their results available to the community, in citable form, before we publish the edited article. This *Accepted Manuscript* will be replaced by the edited, formatted and paginated article as soon as this is available.

You can find more information about *Accepted Manuscripts* in the [Information for Authors](#).

Please note that technical editing may introduce minor changes to the text and/or graphics, which may alter content. The journal's standard [Terms & Conditions](#) and the [Ethical guidelines](#) still apply. In no event shall the Royal Society of Chemistry be held responsible for any errors or omissions in this *Accepted Manuscript* or any consequences arising from the use of any information it contains.

ARTICLE

Layered Perovskite Nanosheets Bearing Fluoroalkoxy Groups: Their Preparation and Application to Epoxy-based Hybrids†

Cite this: DOI: 10.1039/x0xx00000x

Received 00th January 2012,
Accepted 00th January 2012

DOI: 10.1039/x0xx00000x

www.rsc.org/

Yuta Asai,^a Yusuke Ariake,^a Hitomi Saito,^a Naokazu Idota,^b Kimihiro Matsukawa,^c Takashi Nishino^d and Yoshiyuki Sugahara^{*a,b}

Nanosheets bearing $\text{CF}_3(\text{CF}_2)_7\text{C}_2\text{H}_4\text{O}$ groups on their surface were prepared from a $\text{CF}_3(\text{CF}_2)_7\text{C}_2\text{H}_4\text{O}$ derivative of ion-exchangeable layered perovskite $\text{HLaNb}_2\text{O}_7 \cdot x\text{H}_2\text{O}$ (HLaNb) via exfoliation, and were further utilized to prepare epoxy-based hybrids. The $\text{CF}_3(\text{CF}_2)_7\text{C}_2\text{H}_4\text{O}$ derivative of HLaNb (C10F_HLaNb) was prepared by reacting the *n*-decoxy derivative of HLaNb with 1*H*, 1*H*, 2*H*, 2*H*-perfluorodecanol, $\text{CF}_3(\text{CF}_2)_7\text{C}_2\text{H}_4\text{OH}$. TEM and AFM observations revealed that the C10F_HLaNb was exfoliated into individual nanosheets bearing surfaces covered with $\text{CF}_3(\text{CF}_2)_7\text{C}_2\text{H}_4\text{O}$ groups after ultrasonication in acetonitrile. The nanosheet dispersion in acetonitrile was employed to prepare epoxy-based hybrids, and the FE-TEM image of the epoxy-based hybrid with 5 mass% of the nanosheets (C10F_HLaNb/epoxy_5) showed that nanosheets were dispersed in epoxy matrix. Thermogravimetry of C10F_HLaNb/epoxy_5 and neat epoxy resin indicated that the initial mass loss due to water was decreased and thermal decomposition was retarded by introducing C10F_HLaNb nanosheets. Dynamic mechanical thermal analysis revealed that glass transition temperature of C10F_HLaNb/epoxy_5 (161 °C) was higher than that of neat epoxy resin (110 °C). These results clearly exhibit that mechanical and thermal properties were improved by incorporating nanosheets bearing hydrophobic $\text{CF}_3(\text{CF}_2)_7\text{C}_2\text{H}_4\text{O}$ groups in the epoxy resin most likely due to an decrease in water content. Water uptake test demonstrated that water uptake rate of C10F_HLaNb/epoxy_5 was lower than that of the neat epoxy.

Introduction

Nanosheets prepared from layered materials via exfoliation have been attracting increasing attention recently for their potential application in a wide range of fields such as electronics and energy storage.^{1, 2} The compositions of nanosheets, which vary from pure carbon (graphene) to transition metal oxides and dichalcogenides, partly determine their properties. It is of particular interest that the electronic properties of some types of nanosheets, such as those of transition metal oxides and dichalcogenides, can be altered upon exfoliation via changes in their band structures. Their large surface areas are another characteristic that is important for various applications, including capacitors and batteries. Another application for nanosheets is as polymer-based hybrids,³⁻⁶ and various polymer properties, such as their mechanical properties, gas barrier behaviour, and thermal stability, could be drastically improved. A widely recognized example is nylon-clay hybrids (NCH), which exhibit excellent properties.⁷ Smectic clays, typically montmorillonite, have thus been utilized as nanofillers for a variety of polymers besides polyamides,^{8, 9} such as epoxy,¹⁰⁻¹² polyurethane,¹³ polypropylene,¹⁴⁻¹⁶ polyimide¹⁷ and polystyrene.^{18, 19} A reinforcement effect is considered to be the key to improvement

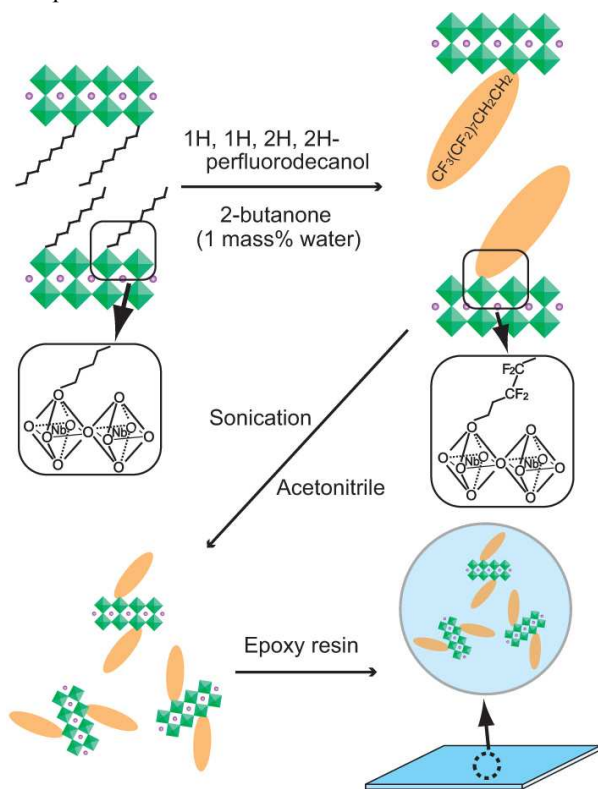
of their mechanical properties.²⁰ Interactions between clay nanosheets and polymer matrices are to play an important role.²¹ It is also generally accepted that incorporation of anisotropic nanosheets improved other properties, such as gas barrier behaviour and flammability resistance.²⁰

Enormous efforts have also been made to utilize synthetic nanosheets, such as layered double hydroxides (LDH),^{22, 23} crystalline layered silicate,²⁴ α -zirconium phosphate,^{15, 25} layered titanate,²⁶ niobate²⁷ and graphene,^{6, 28, 29} in polymer-based hybrids. Possible advantages of the use of these synthetic nanosheets are compositional purity and size control. Among the various methods of exfoliation, on the other hand, liquid exfoliation is suitable for large-scale synthesis² and has thus been extensively applied to the preparation of nanosheets used in polymer-based hybrids.¹ Generally, intercalation and subsequent treatments such as agitation and ultrasonication cause liquid exfoliation.² Since grafting reactions that have been developed for anchoring functional organic groups on the surface of metal oxide particles via covalent bonds^{30, 31} were reported for limited numbers of layered compounds,^{27, 32, 33} it is also possible to prepare exfoliated nanosheets through a combination of grafting reactions and subsequent treatments. The resulting exfoliated organically derivatized nanosheets should exhibit sufficient affinity for organic solvents and

polymers, which is a huge advantage for the preparation of polymer-based hybrids. Another advantage is that surface properties can be easily controlled by the selection of organic groups. So far, a limited number of exfoliated organically derivatized nanosheets has been successfully dispersed in polymers.^{26, 27, 34}

Epoxy resins are known to exhibit a number of excellent properties, including high transparency, good adhesion to various materials and corrosion resistance. Epoxy resins have thus been employed widely in industry, as adhesives,³⁵ coatings³⁶ and packaging materials.³⁷ Enormous efforts have been made to improve their properties further by adding nanosheets, typically clay nanosheets³ as well as such other nanosheets as those synthesized from magadiite²⁴ and α -zirconium phosphate.³⁸ The addition of nanosheets has an effect on many properties, such as cure properties,³⁹ thermal relaxations,⁴⁰ mechanical properties^{10, 11} and water uptake.⁴¹ The improvement of these properties is of particular interest for packaging materials.

We report here the first approach to improve the properties of an epoxy resin by incorporating nanosheets whose surface properties have been changed by modification with fluorinated alcohol, $\text{CF}_3(\text{CF}_2)_7\text{C}_2\text{H}_4\text{OH}$ (C10FOH). As the origin of the nanosheets, a protonated form of ion-exchangeable Dion-Jacobson-type layered perovskite, $\text{HLaNb}_2\text{O}_7 \cdot x\text{H}_2\text{O}$ (HLaNb), was employed after undergoing a direct graft reaction with *n*-decanol,⁴² and the resultant decoxy derivative was used as an intermediate for further reaction with C10FOH in an alcohol-exchange-type reaction. The nanosheets bearing $\text{CF}_3(\text{CF}_2)_7\text{C}_2\text{H}_4\text{O}$ groups were further employed in the epoxy-based hybrids. A detailed characterization of the $\text{CF}_3(\text{CF}_2)_7\text{C}_2\text{H}_4\text{O}$ -derivative of HLaNb (before and after exfoliation) and the behaviour of nanosheet/epoxy hybrids are also reported.



Scheme 1 Overview of the preparation of nanosheets/epoxy hybrids.

Experimental

Materials

HLaNb₂O₇·xH₂O (HLaNb) and its *n*-decoxy derivative (C10_HLaNb) were synthesized by the method reported previously.^{43, 44} Fluorinated alcohol, 1H, 1H, 2H, 2H-perfluorodecanol (C10FOH), was used after purification by recrystallization from hexane. Acetonitrile and 2-butanone were used without further purification. An Epoxy resin, 3, 4-epoxycyclohexylmethyl-3', 4'-epoxycyclohexylcarboxylate (Daicel Chemical Co., Ltd), a mixture of 4-methylhexahydrophthalic anhydride and hexahydrophthalic anhydride (w/w=70/30, New Japan Chemical., Co. Ltd.), which was a curing agent, and triphenylphosphine, which was a curing accelerator, were used without further purification.

Preparation of a $\text{CF}_3(\text{CF}_2)_7\text{C}_2\text{H}_4\text{O}$ derivative of HLaNb

C10_HLaNb, 40 mL of 2-butanone containing 1 mass % of water, and C10FOH were sealed in a glass ampule with C10_HLaNb : C10FOH=1 : 8 (in a molar ratio) and heated at 80 °C for 7 days. The crude product was washed with an excess amount of acetone. After air-drying, the product (denoted as C10F_HLaNb) was obtained.

Exfoliation of C10F_HLaNb

To obtain a suspension, 0.1 g of C10F_HLaNb was dispersed in 50 mL of acetonitrile and sonicated for 1 h (Digital Sonifier, BRANSON Ltd.) in an ice bath. After centrifugation (4000 rpm, 15 min) and removing precipitate, nanosheets (denoted as C10F_HLaNb_NS) dispersed in acetonitrile were prepared.

Preparation of epoxy-based hybrids

A stoichiometric mixture of the epoxy resin and the curing agent (w/w=134 : 164), and triphenylphosphine (corresponding to 0.5 mass% of the epoxy content), were added to the nanosheet dispersion. The polymer concentrations of these solutions were adjusted to 20 mass% by diluting with acetonitrile. The mixture was stirred and deformed for 30 min each. Then, the mixture was cast on the polyethylene terephthalate (PET) substrate with bar-coated (90 μm gap). The product was then cured at 80 °C for 1 day, and postcured at 90 °C for 4 h. Epoxy-based hybrids incorporating C10F_HLaNb_NS were denoted as C10F_HLaNb/epoxy_x (x is content of nanosheets to the epoxy in mass%).

Instrumentation

X-ray diffraction (XRD) patterns were obtained with a Rigaku RINT-1100 diffractometer (FeK α radiation). Infrared (IR) spectra were recorded on a JASCO FT/IR-460 Plus spectrometer using the KBr method. Solid-state ¹³C nuclear magnetic resonance (NMR) spectra were obtained with a JEOL ECX-400 spectrometer at 100.54 MHz with cross-polarization (CP) and magic angle spinning (MAS) techniques (pulse delay, 5s; contact time, 5 ms; spinning rate, 10 kHz). Scanning

electron microscopic (SEM) observation was performed with a JEOL JSM-5600 microscope operating at 15 kV. The compositions of metals were determined by inductively coupled plasma (ICP) emission spectrometry using a Varian VISTA-MPX CCD simultaneous ICP-OES instrument after dissolving the samples (about 10 mg) in a mixture of 5 mL of HNO₃ (69–70 mass%), 5 mL of H₂SO₄ (>96 mass%), and 10 mL of HF (46–48 mass%) at 200 °C for 2 h. CHN analysis was performed with a PERKIN ELMER PE2400 instrument. X-ray fluorescence spectroscopy (XRF) was performed with a Rigaku ZSX Primus II instrument.

Transmission electron microscopic (TEM) images were obtained with a JEOL JEM-1011 microscope operating at 100 kV. TEM samples were prepared by dropping a droplet of the nanosheet dispersion on a carbon supported copper mesh TEM grid and subsequently acetonitrile was evaporated. Atomic force microscope (AFM) observation was performed on a Digital Instruments Multimode AFM Nanoscope III microscope. An AFM sample was prepared by evaporating acetonitrile of the nanosheet dispersion on a silicon wafer.

Optical microscopic observation was performed on a KEYENCE VK-9500 microscope. UV-Vis spectra were measured on a JASCO V-630 UV-Vis spectrometer in the range of 400–800 nm. Field emission transmission electron microscopy (FE-TEM) was performed on a JEOL JEM-2100F microscope operating at 200 kV. For preparation of a sample, an epoxy-based hybrid was prepared on a Si wafer and an ultrathin section of the film was cut by a focused ion beam instrument (SEIKO EG&G SMI 2050). The epoxy conversions were estimated by IR spectra,³⁸ in which a band due to the epoxy group and a C=O stretching band of ester were observed at 790 and 1760 cm⁻¹, respectively. The absorbance ratios of the epoxy group band to the ester group band in the samples were

normalized by the absorbance ratio of the raw material, and the decrease in the normalized absorbance ratio indicates the proceeding of epoxy conversion.

For dynamic mechanical thermal analysis (DMTA), specimens with dimensions of 30 mm (length) × 5 mm (width) × 100 μm (thickness) were prepared. Dynamic mechanical analysis was performed with a DVA-220S dynamic mechanical thermal analyzer (ITK Ltd.) at a heating rate of 6 K/min and a frequency of 10 Hz. A tensile deformation of 0.25% was applied to the sample, and the temperature of the most intense relaxation peak on the tan δ versus temperature curve was defined as glass transition temperature (*T_g*). Thermogravimetry (TG) was performed with a PERKIN ELMER TGA7 thermobalance in the temperature range from 30 to 600 °C at a heating rate of 10 °C/min under an air flow. For water uptake measurements, specimens were prepared on the 3 × 3 cm PET substrate. Then, the specimens were immersed in water at 30 °C. The specimens were weighed periodically after drying with a paper towel to remove excessive surface water. Water uptake rate, *M_t*, was calculated by the following formula,

$$M_t = \frac{W_t - W_1}{W_1} \times 100 \quad (\text{Eq. 1})$$

where, *W_t* is the weight of specimens immersed in water and *W₁* is the initial weight of dried specimens.

Results and discussion

Preparation of a CF₃(CF₂)₇C₂H₄O derivative of HLaNb

Figure 1 shows the XRD patterns of C10_HLaNb and the product of the reaction between C10_HLaNb and C10FOH (C10F_HLaNb). In the XRD pattern of C10F_HLaNb, the diffraction line corresponding to the interlayer distance of C10_HLaNb (*d* = 2.75 nm) disappears and a new diffraction line appears at *d* = 3.30 nm. On the other hand, (100) and (110) reflections of HLaNb do not shift in the both patterns, indicating that structure of the perovskite-like slabs is retained after the reaction.

The solid-state ¹³C CP/MAS NMR spectrum of C10F_HLaNb is demonstrated in Figure 2c. In the spectrum, signals assignable to CF₃(CF₂)₇C₂H₄O moieties are present at 119 (CF₃-), 112 (CF₃-(CF₂)₇-), 35 (-(CF₂)₇-CH₂-), and 72 (-(CF₂)₇-CH₂-CH₂-O-) ppm.⁴⁵ As compared to the α-carbon signal of C10FOH at 55 ppm (shown in Figure 2b), the α-carbon signal shifts downfield to 72 ppm by 17 ppm. It was reported that α-carbon signals shifted downfield by about 17 ppm from the signal positions of the corresponding alcohols in the spectra of *n*-alkoxy derivatives of HLaNb.⁴⁴ It is thus concluded that C10FOH is grafted onto the surface of HLaNb as an CF₃(CF₂)₇C₂H₄O groups via alcohol-exchange type reactions.⁴⁴ On the other hand, signals at 82, 26, 23, 12 ppm can be assignable to *n*-deoxy groups. The presence of these signals indicates that alcohol-exchange reaction between C10_HLaNb and C10FOH does not complete.

In the IR spectrum of C10F_HLaNb (Figure S1 in the ESI), C-H stretching bands (2963 cm⁻¹, *v*_{as}(CH₃); 2933 cm⁻¹, *v*_{as}(CH₂);

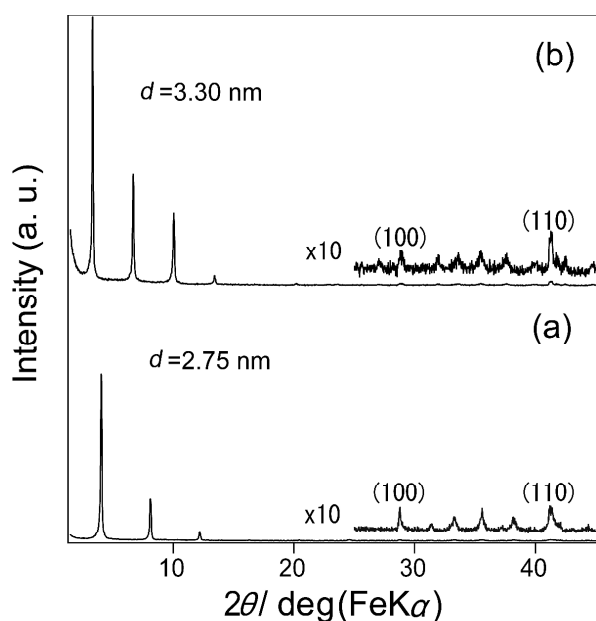


Fig. 1 XRD patterns of (a) C10_HLaNb and (b) C10F_HLaNb.

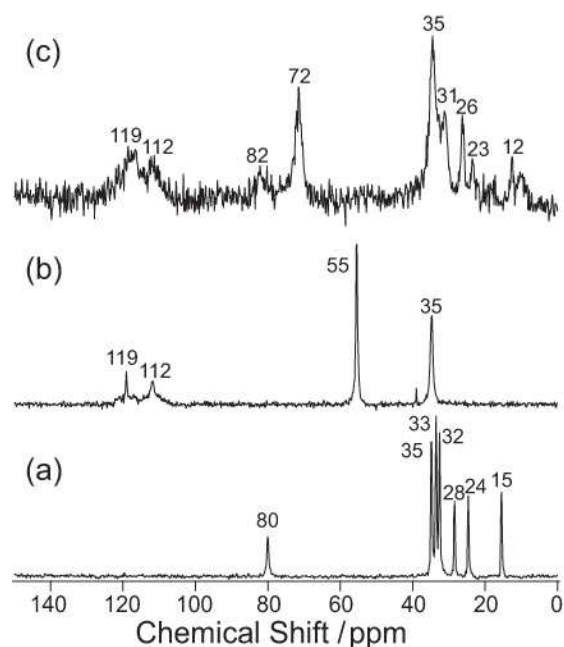


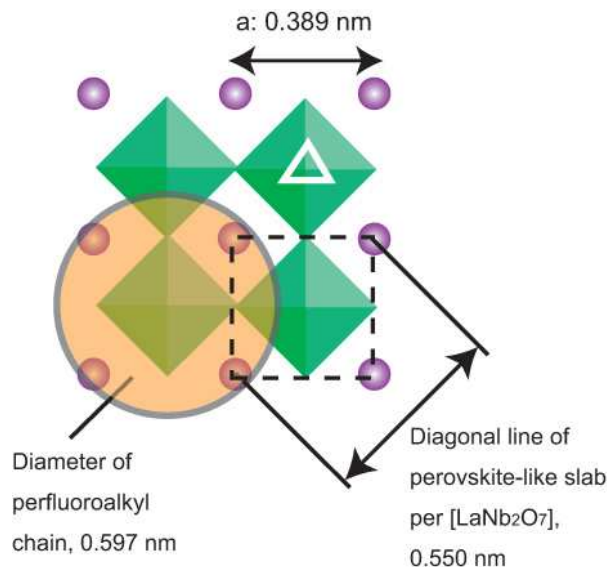
Fig. 2 ^{13}C CP/MAS NMR spectra of (a) C10_HLaNb, (b) C10FOH and (c) C10F_HLaNb.

2880 cm^{-1} , ν_{s} (CH_3); 2860 cm^{-1} , ν_{s} (CH_2), CH_2 bending band (1468 cm^{-1}), C-F stretching bands⁴⁶ (1204 cm^{-1} , ν_{as} (CF_2); 1148 cm^{-1} , ν_{s} (CF_2)), and C-O stretching band (1116 cm^{-1}), are observed. In particular, the presence of C-F stretching bands suggests that $\text{CF}_3(\text{CF}_2)_7\text{C}_2\text{H}_4\text{O}$ groups are present in C10F_HLaNb. On the other hand, weak absorption bands due to ν_{as} (CH_3) and ν_{s} (CH_3) modes, which are absent in the spectrum of C10FOH, are observed, suggesting that a part of *n*-decoxy groups remains, results consistent with the NMR results.

The molar ratios of Nb and La are calculated from the ICP results, and La/Nb ratios are 0.5 for C10F_HLaNb and C10_HLaNb. In addition, SEM images of C10_HLaNb and C10F_HLaNb (Figure S2 in the ESI) reveal that both products exhibit essentially the same plate-like morphology. These results suggest that the structure of perovskite-like slabs is preserved during the reaction of C10_HLaNb and C10FOH.

The amounts of $\text{CF}_3(\text{CF}_2)_7\text{C}_2\text{H}_4\text{O}$ and *n*-decoxy groups grafted to HLaNb are calculated from CHN analysis and XRF results; $\text{CF}_3(\text{CF}_2)_7\text{C}_2\text{H}_4\text{O}$ groups in C10F_HLaNb are 0.43 per $[\text{LaNb}_2\text{O}_7]$, while unreacted *n*-decoxy groups in C10F_HLaNb are 0.10 per $[\text{LaNb}_2\text{O}_7]$. The diameter of $\text{CF}_3(\text{CF}_2)_7\text{C}_2\text{H}_4\text{O}$ chain, 0.597 nm,⁴⁷ is larger than the diagonal distance of the unit cell along the *ab* plane of $[\text{LaNb}_2\text{O}_7]$, 0.550 nm, the distance between two (HO)NbO₅ sites as shown in Scheme 2. When one (HO)NbO₅ site reacts with C10FOH, the nearest site, indicated by a white triangle, cannot react with C10FOH, leading to the maximal amount of $\text{CF}_3(\text{CF}_2)_7\text{C}_2\text{H}_4\text{O}$ groups per $[\text{LaNb}_2\text{O}_7]$ to be 0.5. Since the diameter of *n*-alkyl chain (0.486 nm)⁴⁸ is much smaller, it is possible that both $\text{CF}_3(\text{CF}_2)_7\text{C}_2\text{H}_4\text{O}$ and *n*-decoxy groups are present at the two nearest sites [0.597+0.486 nm < 0.550+0.550 nm]. Thus unhydrolyzed *n*-decoxy groups can be present among $\text{CF}_3(\text{CF}_2)_7\text{C}_2\text{H}_4\text{O}$ - groups.

It should be noted that in the solid-state ^{13}C CP/MAS NMR spectrum of C10F_HLaNb, signals of *n*-decoxy groups are emphasized, since only limited amount of hydrogen atoms are present in $\text{CF}_3(\text{CF}_2)_7\text{C}_2\text{H}_4\text{O}$ groups.



Scheme 2 Relationships between the length of the HO-NbO₅ site and that of the fluoroalkoxy chain.

Exfoliation of C10F_HLaNb

Figure 3 shows TEM images of the $\text{CF}_3(\text{CF}_2)_7\text{C}_2\text{H}_4\text{O}$ derivative of HLaNb before and after ultrasonication in acetonitrile (C10F_HLaNb and C10F_HLaNb_NS). After ultrasonication, plate-like morphology with light contrast is observed in comparison with that of C10F_HLaNb, indicating that exfoliation occurs, and their lateral sizes are mostly in range of 100-200 nm. The electron diffraction pattern of C10F_HLaNb_NS (the inset of Figure 3b) is single-crystal-type, which can be indexed as tetragonal cell with $a = 0.39$ nm, a result consistent with layered perovskite structure.⁴³ It is thus concluded that the structure of perovskite-like slabs is not changed after exfoliation.

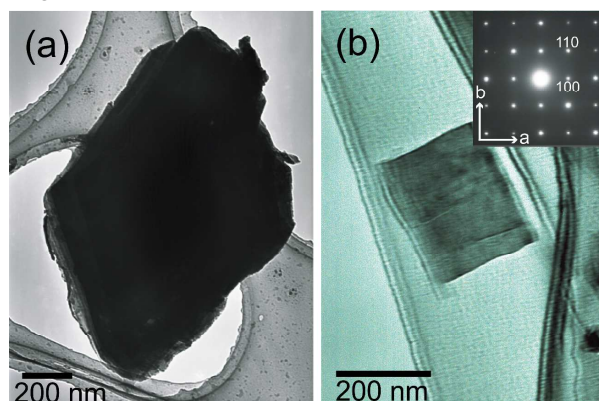


Fig. 3 TEM images of C10F_HLaNb (a) before the ultrasonication and (b) after the ultrasonication (C10F_HLaNb_NS).

AFM image of C10F_HLaNb_NS is demonstrated in Figure 4. Plate-like morphology is also observed and its height profile shows the thickness of 3.3 nm along the scanned line. Since the interlayer distance of C10F_HLaNb, before exfoliation, is 3.30 nm, which contain the thickness of [LaNb₂O₇] and doubled thickness of CF₃(CF₂)₇C₂H₄O layers. It is thus assumed that obtained C10F_HLaNb_NS consists of a monolayer which possesses CF₃(CF₂)₇C₂H₄O groups on both side of the layer.

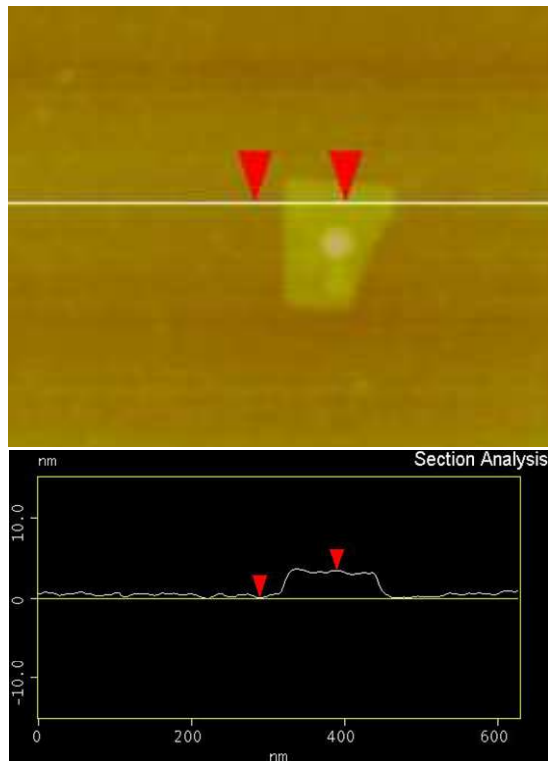


Fig. 4 AFM image of C10F_HLaNb_NS and height profile on the white line.

Preparation of epoxy-based hybrids

Nanosheet/epoxy hybrids prepared were transparent and colorless films, which were similar to the neat epoxy film, were obtained. In addition, optical microscopic observation reveals that these films have neither crack nor pinhole on their surfaces (Figure S3 in the ESI). The epoxy conversions of neat epoxy resin and C10F_HLaNb/epoxy_5 were 47.6 and 51.7%, respectively. The incorporation of 5 mass% modified nanosheets thus did not affect the epoxy curing behaviour.

UV-Vis spectra of these films are shown on Figure S4 in the ESI. Transmittance values at 633 nm are 100% (neat epoxy) and 91% (C10F_HLaNb/epoxy_5). Previous studies on montmorillonite/epoxy hybrids, which have been widely explored, demonstrated that transmittance values of epoxy-based hybrids with 5 mass% of nanosheets were in range of 47-92%,⁴⁹⁻⁵¹ indicating that transparency of epoxy-based hybrid in the present study is excellent.

Dispersion of epoxy-based hybrid is studied by FE-TEM image of cross sections of C10F_HLaNb/epoxy_5 (Figure 5).

The dark lines, whose thickness is ~ 1 nm, represent monolayer nanosheets. TEM observations show that essentially all of the modified nanosheets are exfoliated, and dispersed in epoxy matrix.

Properties of epoxy-based hybrids

Thermal properties of epoxy-based hybrids were evaluated with thermogravimetry (TG) and dynamic mechanical thermal analysis (DMTA). Figure 6 shows TG curves of neat epoxy and

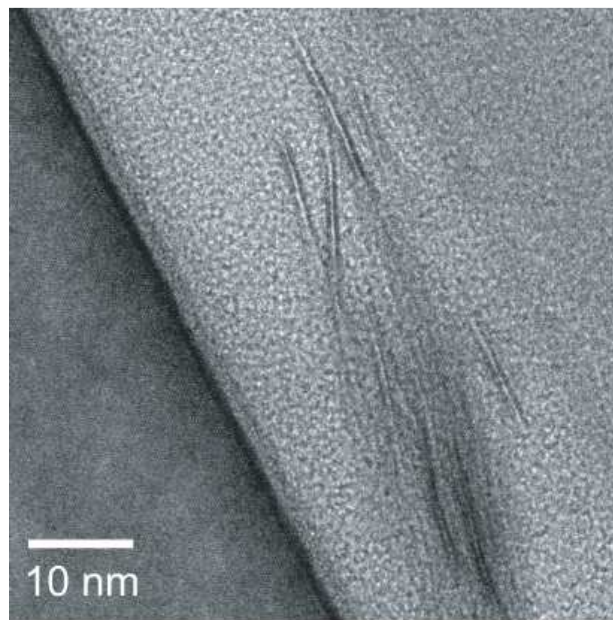


Fig. 5 Cross-section FE-TEM image of C10F_HLaNb/epoxy_5.

epoxy-based hybrids. Two noticeable differences are clearly shown upon comparison. One difference is in initial mass loss region assignable to loss of water, and the TG curve of C10F_HLaNb/epoxy_5 exhibits a much smaller initial mass loss, results indicating the presence of a smaller amount of water in C10F_HLaNb/epoxy_5. The other difference is above 200 °C, where degradation of epoxy resin occurs. The steep mass loss in the TG curve of C10F_HLaNb/epoxy_5 shifts to high temperature compared to that of neat epoxy. Temperatures at which 30 % degradation occurs ($T_{30\%}$) are 311 °C (C10F_HLaNb/epoxy_5) and 284 °C (neat epoxy) (Table 1). In general, water sorption in epoxy resin leads to reduced thermal stability because of the plasticizing effect, chain scission and decreasing cross linking density of epoxy resin.⁵² In this study, it is assumed that C10F_HLaNb/epoxy_5 contains a less amount of water because of the presence of hydrophobic nanosheets bearing CF₃(CF₂)₇C₂H₄O groups on the surface, leading to high cross linking density of epoxy and consequently to high T_g and $T_{30\%}$.

$T_{30\%}$ values of epoxy-based hybrids with different C10F_HLaNb_NS contents are listed in Table 1. Based on the comparison between $T_{30\%}$ values of 10F_HLaNb/epoxy_3 and C10F_HLaNb/epoxy_5, it is demonstrated that C10F_HLaNb/epoxy_5 exhibit better thermal stability than neat epoxy but inferior to C10F_HLaNb/epoxy_5. The $T_{30\%}$ value is

lower, even compared to that of neat epoxy (284 °C), however, when 7 mass% of nanosheets are loaded (C10F_HLaNb/epoxy_7, 272 °C). It is known that the addition of an excess amount of nanosheets decreases the curing reactivity of epoxy resin.⁵³ In fact, the epoxy conversion of C10F_HLaNb/epoxy_7 was estimated to be 34.0%, which is a much smaller ratio than those of neat epoxy and epoxy-based hybrids with 5 mass% modified nanosheets (~50%). Lower reactivity leads to lower cross-linking density, which makes epoxy resin thermally less stable. In the case of C10F_HLaNb/epoxy_7, thermal stability deteriorated because this effect would be dominant.

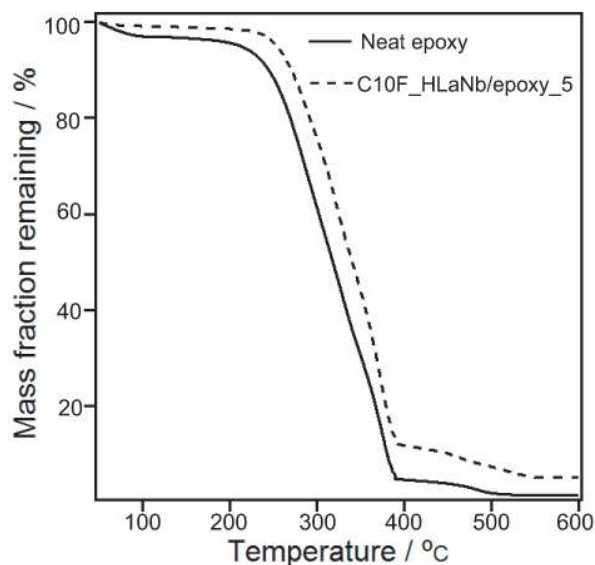


Fig. 6 Mass loss curves of neat epoxy and C10F_HLaNb/epoxy_5.

Table 1 The effect of the C10F_HLaNb_NS content on decomposition temperatures of 30% mass loss.

Sample	$T_{30\%}$ / °C
Neat epoxy	284
C10F_HLaNb/epoxy_3	296
C10F_HLaNb/epoxy_5	311
C10F_HLaNb/epoxy_7	272

DMTA curves of neat epoxy and epoxy-based hybrid were measured to investigate the effect of incorporation of modified nanosheets in epoxy resin (Figure 7). In order to exclude the effect of the epoxy conversion, C10F_HLaNb/epoxy_5 was used as a hybrid sample. Transitions between glass and rubber states in neat and C10F_HLaNb/epoxy are observed by the sigmoid curves of storage modulus (E') depended on temperature, and the changes in $\tan \delta$ indicated higher T_g of C10F_HLaNb/epoxy_5 than that of neat epoxy (110 °C for neat epoxy to 161 °C for C10F_HLaNb/epoxy_5). The T_g values of neat epoxy in this study were lower than those reported previously for epoxy resins based on 3, 4-epoxycyclohexylmethyl-3', 4'-epoxycyclohexyl carboxylate (>

200 °C).³⁸ Meyer *et al.* reported that the highest T_g of epoxy resin was achieved in the stoichiometric formulation given by a high curing temperature.⁵⁴ Thus, the low T_g was a result of the lower curing temperature employed in the present study. In addition, the epoxy resin in the feed in the present study contained acetonitrile, which was used as a dispersion medium for modified nanosheets. Thus, a low curing temperature and the presence of acetonitrile may lead to a reduced degree of cross-linkage in an epoxy network, resulting in low T_g . T_g is also dependent on the amount of water by the aforementioned plasticizing effect. It was proposed that water molecules enhanced the chain segment mobility of epoxy resin by breaking the van der Waals forces and hydrogen bonds between polymer chains, resulting in reduction of T_g .⁵⁵ In addition, the obvious broaden shoulder peak of $\tan \delta$ (at 50 °C for neat epoxy) disappears in the curve of C10F_HLaNb. De'Nève *et al.* indicated that decrease in T_g of epoxy resin and a split in the peak of $\tan \delta$ were observed due to the presence of water which were not linked to the polymer network chemically.⁵⁶ In the present results, E' values of C10F_HLaNb/epoxy_5 at rubber region are larger than those of neat epoxy, whereas very similar E' values were observed for C10F_HLaNb/epoxy_5 and neat epoxy at glass region. It was reported that the decrease in E' values in the rubber region was caused by polymer chain scission resulting from humid aging, which is caused by exposure of epoxy resin to an atmosphere of ca. 100% humidity.⁵⁶ Thus, the dispersion of C10F_HLaNb nanosheets in an epoxy matrix would improve its thermal properties by reducing the amount of water.

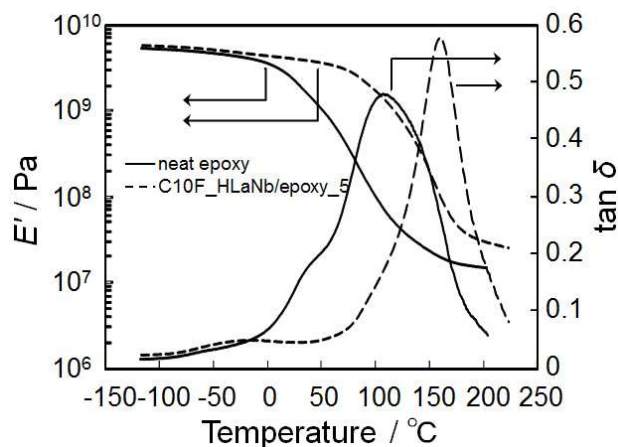


Fig. 7 Temperature dependence of the dynamic E' and $\tan \delta$ of neat epoxy and C10F_HLaNb/epoxy_5.

Figure 8 shows water uptake curves of neat epoxy and C10F_HLaNb/epoxy_5. It is clearly revealed that C10F_HLaNb/epoxy_5 absorbs a less amount of water than neat epoxy. The water uptake rate (M_t) value of C10F_HLaNb/epoxy_5 after 4 days corresponds to 71% M_t value of neat epoxy after 4 days, and the decrease of water uptake rate is ascribable to the barrier effect of nanosheets in epoxy resin which increase the diffusion path of water.^{41, 49} In addition, it should be noted that M_t of C10F_HLaNb/epoxy_5 is

lower than those in previous reports of epoxy-based hybrids, whose M_t in range of 80-95 % compared to neat epoxy resin.⁴¹ It is thus likely that the highly hydrophobic $\text{CF}_3(\text{CF}_2)_7\text{C}_2\text{H}_4\text{O}$ groups also contribute to lowering water uptake. As a result, C10F_HLaNb/epoxy_5 shows excellent water resistance.

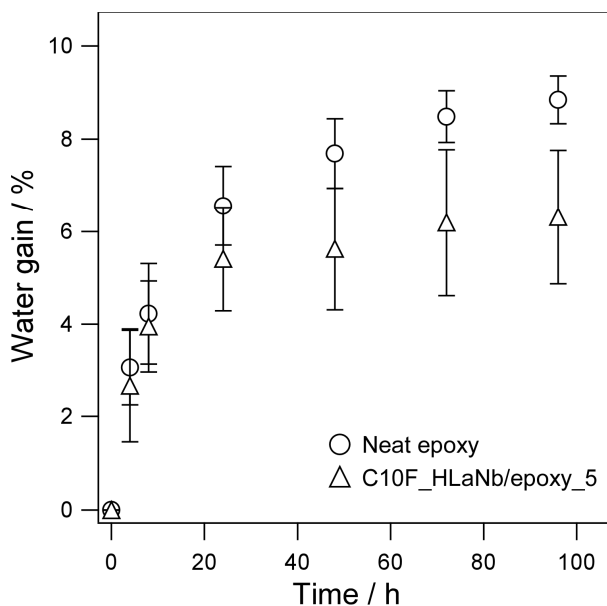


Fig. 8 Water absorption curves of neat epoxy and C10F_HLaNb/epoxy_5.

Conclusions

Nanosheets bearing hydrophobic $\text{CF}_3(\text{CF}_2)_7\text{C}_2\text{H}_4\text{O}$ groups on the surface were prepared via exfoliation of a $\text{CF}_3(\text{CF}_2)_7\text{C}_2\text{H}_4\text{O}$ -derivative of $\text{HLaNb}_2\text{O}_7 \cdot x\text{H}_2\text{O}$ (C10F_HLaNb) by ultrasonication in acetonitrile, and highly transparent epoxy-based hybrids where $\text{CF}_3(\text{CF}_2)_7\text{C}_2\text{H}_4\text{O}$ -bearing nanosheets were dispersed were prepared. When 5 mass% of nanosheets were loaded to epoxy resin, mechanical and thermal properties were improved. Water uptake rate was also reduced compared to that of neat epoxy resin. Although the previous nanosheet/polymer hybrids utilized nanosheets bearing original surfaces, the present results clearly demonstrate that the use of surface modified nanosheets is advantageous for preparing polymer-based hybrids with improved properties.

Acknowledgments

This work was financially supported in part by a Grant-in-Aid for Scientific Research on Innovative Areas “New Polymeric Materials Based on Element-Blocks (No. 2401)” (24102002), and the Global COE program “Center for Practical Chemical Wisdom” of the Ministry of Education, Culture, Sports, Science, and Technology, Japan. The authors thank Daicel Chemical Co., Ltd. for donating 3, 4-epoxycyclohexylmethyl-3', 4'-epoxycyclohexylcarboxylate. They also thank Mr. Yuhi Shibuya and Mr. Mineichi Fujiwara, Kagami Memorial Research Institute for Materials Science and Technology in

Waseda University, for their support for FE-TEM observation, and Ms. Maiko Ariyoshi, Department of Chemical Science and Engineering in Kobe University, for her support for dynamic mechanical thermal analysis.

Notes and references

^a Department of Applied Chemistry, School of Science and Engineering, Waseda University, Okubo-3, Shinjuku-ku, Tokyo 169-8555, Japan.

^b Kagami Memorial Research Institute for Materials Science and Technology, Waseda University, Nishiwaseda-2, Shinjuku-ku, Tokyo, Japan.

^c Osaka Municipal Technical Research Institute, Morinomiya-1, Joto-ku, Osaka 536-8553, Japan.

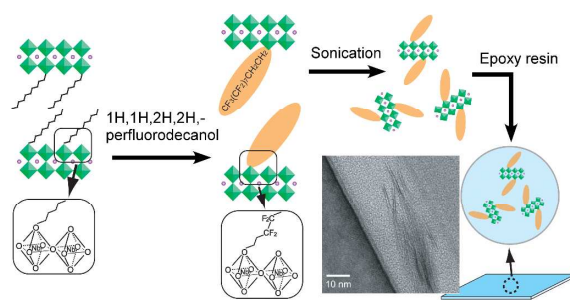
^d Department of Chemical Science and Engineering, Graduate School of Engineering, Kobe University, Rokkodai-1, Nada-ku, Kobe 657-8501, Japan

* E-mail: ys6546@waseda.jp; Fax: +81-3-5286-3204; Tel: +81-3-5286-3204

† Electronic Supplementary Information (ESI) available. See DOI: 10.1039/b000000x/

- J. N. Coleman, M. Lotya, A. O'Neill, S. D. Bergin, P. J. King, U. Khan, K. Young, A. Gaucher, S. De, R. J. Smith, I. V. Shvets, S. K. Arora, G. Stanton, H. Y. Kim, K. Lee, G. T. Kim, G. S. Duesberg, T. Hallam, J. J. Boland, J. J. Wang, J. F. Donegan, J. C. Grunlan, G. Moriarty, A. Shmeliov, R. J. Nicholls, J. M. Perkins, E. M. Grieveson, K. Theuvsen, D. W. McComb, P. D. Nellist and V. Nicolosi, *Science*, 2011, **331**, 568-571.
- V. Nicolosi, M. Chhowalla, M. G. Kanatzidis, M. S. Strano and J. N. Coleman, *Science*, 2013, **340**, 1226419-1226419.
- P. C. LeBaron, Z. Wang and T. J. Pinnavaia, *Applied Clay Science*, 1999, **15**, 11-29.
- C. Sanchez, G. J. d. A. A. Soler-Illia, F. Ribot, T. Lalot, C. R. Mayer and V. Cabuil, *Chem. Mater.*, 2001, **13**, 3061-3083.
- G. Schmidt and M. M. Malwitz, *Curr. Opin. Colloid Interface Sci.*, 2003, **8**, 103-108.
- R. Sengupta, M. Bhattacharya, S. Bandyopadhyay and A. K. Bhowmick, *Prog. Polym. Sci.*, 2011, **36**, 638-670.
- A. Usuki, Y. Kojima, M. Kawasumi, A. Okada, Y. Fukushima, T. Kurauchi and O. Kamigaito, *J. Mater. Res.*, 1993, **8**, 1179-1184.
- X. H. Liu and Q. J. Wu, *Macromol. Mater. Eng.*, 2002, **287**, 180-186.
- A. D. Liu, T. X. Xie and G. S. Yang, *Macromol. Chem. Phys.*, 2006, **207**, 701-707.
- T. Lan and T. J. Pinnavaia, *Chem. Mater.*, 1994, **6**, 2216-2219.
- T. Lan, P. D. Kaviratna and T. J. Pinnavaia, *Chem. Mater.*, 1995, **7**, 2144-2150.
- P. B. Messersmith and E. P. Giannelis, *Chem. Mater.*, 1994, **6**, 1719-1725.
- Z. Wang and T. J. Pinnavaia, *Chem. Mater.*, 1998, **10**, 3769-+.
- M. Kato, A. Usuki and A. Okada, *J. Appl. Polym. Sci.*, 1997, **66**, 1781-1785.
- H. J. Sue, K. T. Gam, N. Bestaoui, N. Spurr and A. Clearfield, *Chem. Mater.*, 2004, **16**, 242-249.
- Y. Kurokawa, H. Yasuda and A. Oya, *J. Mater. Sci. Lett.*, 1996, **15**, 1481-1483.

17. K. Yano, A. Usuki and A. Okada, *J. Polym. Sci. A-Polym. Chem.*, 1997, **35**, 2289-2294.
18. A. Akelah and A. Moet, *Journal of Materials Science*, 1996, **31**, 3589-3596.
19. T. L. Porter, M. E. Hagerman, B. P. Reynolds, M. P. Eastman and R. A. Parnell, *J. Polym. Sci. B-Polym. Phys.*, 1998, **36**, 673-679.
20. D. R. Paul and L. M. Robeson, *Polymer*, 2008, **49**, 3187-3204.
21. N. Bitinis, M. Hernandez, R. Verdejo, J. M. Kenny and M. A. Lopez-Manchado, *Adv. Mater.*, 2011, **23**, 5229-5236.
22. F. R. Costa, M. Abdel-Goad, U. Wagenknecht and G. Heinrich, *Polymer*, 2005, **46**, 4447-4453.
23. Q. Wang and D. O'Hare, *Chem. Rev.*, 2012, **112**, 4124-4155.
24. Z. Wang and T. J. Pinnavaia, *Chem. Mater.*, 1998, **10**, 1820-1826.
25. Y. J. Yang, C. H. Liu and H. X. Wu, *Polym. Test.*, 2009, **28**, 371-377.
26. Y. Fuse, Y. Ide and M. Ogawa, *Polym. Chem.*, 2010, **1**, 849-853.
27. N. Kimura, Y. Kato, R. Suzuki, A. Shimada, S. Tahara, T. Nakato, K. Matsukawa, P. H. Mutin and Y. Sugahara, *Langmuir*, 2014, **30**, 1169-1175.
28. G. H. Chen, C. L. Wu, W. G. Weng, D. J. Wu and W. L. Yan, *Polymer*, 2003, **44**, 1781-1784.
29. T. Ramanathan, A. A. Abdala, S. Stankovich, D. A. Dikin, M. Herrera-Alonso, R. D. Piner, D. H. Adamson, H. C. Schniepp, X. Chen, R. S. Ruoff, S. T. Nguyen, I. A. Aksay, R. K. Prud'homme and L. C. Brinson, *Nat. Nanotechnol.*, 2008, **3**, 327-331.
30. P. VanDerVoort and E. F. Vansant, *J. Liquid Chromatogr. Related Technol.*, 1996, **19**, 2723-2752.
31. P. H. Mutin, G. Guerrero and A. Vioux, *C. R. Chim.*, 2003, **6**, 1153-1164.
32. Y. Mitamura, Y. Komori, S. Hayashi, Y. Sugahara and K. Kuroda, *Chem. Mater.*, 2001, **13**, 3747-3753.
33. E. Ruiz-Hitzky, *Chem. Rec.*, 2003, **3**, 88-100.
34. T. Takei, Q. A. Dong, Y. Yonesaki, N. Kumada and N. Kinomura, *Langmuir*, 2011, **27**, 126-131.
35. D. F. S. Saldanha, C. Canto, L. F. M. da Silva, R. J. C. Carbas, F. J. P. Chaves, K. Nomura and T. Ueda, *Int. J. Adhes. Adhes.*, 2013, **47**, 91-98.
36. J. Simal-Gándara, S. Paz-Abuín and L. Ahrné, *Crit. Rev. Food Sci. Nutr.*, 1998, **38**, 675-688.
37. Y. Zhang, M. Cao, G. Guo, J. Sun, Z. Li, P. Xie, R. Zhang and P. Fu, *J. Mater. Chem.*, 2002, **12**, 2325-2330.
38. R. Bongiovanni, M. Casciola, A. Di Gianni, A. Donnadio and G. Malucelli, *Eur. Polym. J.*, 2009, **45**, 2487-2493.
39. P. J. Halley and M. E. Mackay, *Polym. Eng. Sci.*, 1996, **36**, 593-609.
40. I. Zaman, Q. H. Le, H. C. Kuan, N. Kawashima, L. Luong, A. Gerson and J. Ma, *Polymer*, 2011, **52**, 497-504.
41. O. Becker, R. J. Varley and G. P. Simon, *Eur. Polym. J.*, 2004, **40**, 187-195.
42. S. Takahashi, T. Nakato, S. Hayashi, Y. Sugahara and K. Kuroda, *Inorg. Chem.*, 1995, **34**, 5065-5069.
43. J. Gopalakrishnan, V. Bhat and B. Raveau, *Mater. Res. Bull.*, 1987, **22**, 413-417.
44. H. Suzuki, K. Notsu, Y. Takeda, W. Sugimoto and Y. Sugahara, *Chem. Mater.*, 2003, **15**, 636-641.
45. Q. Chen and K. Schmidt-Rohr, *Macromolecules*, 2004, **37**, 5995-6003.
46. M. H. Lee, T. H. Ha and K. Kim, *Langmuir*, 2002, **18**, 2117-2124.
47. H. Lebreton, B. Bennetau, J. Dunogues, J. F. Letard, R. Lapouyade, L. Vignau and J. P. Morand, *Langmuir*, 1995, **11**, 1353-1360.
48. A. Goni, J. Rius, M. Insausti, L. M. Lezama, J. L. Pizarro, M. I. Arriortua and T. Rojo, *Chem. Mater.*, 1996, **8**, 1052-1060.
49. K. H. Chen and S. M. Yang, *J. Appl. Polym. Sci.*, 2002, **86**, 414-421.
50. Y. M. Deng and A. J. Gu, *Polym.-Plastics Technol. Eng.*, 2003, **42**, 899-910.
51. I. N. Jan, T. M. Lee, K. C. Chiou and J. J. Lin, *Ind. Eng. Chem. Res.*, 2005, **44**, 2086-2090.
52. K. I. Ivanova, R. A. Pethrick and S. Affrossman, *Polymer*, 2000, **41**, 6787-6796.
53. A. J. Gu and G. Z. Liang, *Polym. Degrad. Stabil.*, 2003, **80**, 383-391.
54. F. Meyer, G. Sanz, A. Eceiza, I. Mondragon and J. Mijović, *Polymer*, 1995, **36**, 1407-1414.
55. J. Zhou and J. P. Lucas, *Polymer*, 1999, **40**, 5513-5522.
56. B. De'Nève and M. E. R. Shanahan, *Polymer*, 1993, **34**, 5099-5105.



Highlight: Nanosheets bearing fluoroalkoxy groups were prepared via exfoliation of a $\text{CF}_3(\text{CF}_2)_7\text{C}_2\text{H}_4\text{O}$ derivative of $\text{HLaNb}_2\text{O}_7 \cdot x\text{H}_2\text{O}$ for application to epoxy-based hybrids.